AIP Advances

Chimera states induced by spike timing-dependent plasticity in a regular neuronal network

Cite as: AIP Advances **12**, 105119 (2022); https://doi.org/10.1063/5.0101055
Submitted: 28 May 2022 • Accepted: 24 September 2022 • Published Online: 27 October 2022

Chao Yang, Moises S. Santos, Paulo R. Protachevicz, et al.

Chimera states induced by spike timing-dependent plasticity in a regular neuronal network

Cite as: AIP Advances 12, 105119 (2022); doi: 10.1063/5.0101055
Submitted: 28 May 2022 • Accepted: 24 September 2022 •
Published Online: 27 October 2022

Chao Yang,[1,a] Moises S. Santos,[2] Paulo R. Protachevicz,[2] Patrício D. C. dos Reis,[3] Kelly C. Iarosz,[4,5] Iberê L. Caldas,[2] and Antonio M. Batista[3,6,b]

AFFILIATIONS

[1] School of Information Science and Technology, Fudan University, 200433 Shanghai, China
[2] Physics Institute, University of São Paulo, 05508-090 São Paulo, Brazil
[3] Postgraduate Program in Sciences, State University of Ponta Grossa, Ponta Grossa, Paraná 84030-900, Brazil
[4] University Center UNIFATEB, Telêmaco Borba, Paraná 84266-010, Brazil
[5] Graduate Program in Chemical Engineering Federal Technological University of Paraná, Ponta Grossa, Paraná 84017-220, Brazil
[6] Department of Mathematics and Statistics, State University of Ponta Grossa, Ponta Grossa, Paraná 84030-900, Brazil

[a] **Electronic mail:** 20210720076@fudan.edu.cn
[b] **Author to whom correspondence should be addressed:** abatista@uepg.br

ABSTRACT

Chimera states are spatiotemporal patterns in which distinct dynamics coexist, such as synchronous and asynchronous patterns. In this work, we study the effect of spike timing-dependent plasticity (STDP) on the emergence of chimera states. We consider a regular network of coupled adaptive exponential integrate-and-fire neurons, where all connections initially have the same strength value. The STDP alters the strength value as a function of the timing between the pre and postsynaptic action potentials over time. We verify that the range of parameters displaying chimera states is larger in the network with plasticity than in the absence of plasticity. Our simulations show that the chimera lifetime increases when the plasticity actuates in the neuronal network. We also observe an increase in neuronal spike frequency when the neurons are submitted to a constant positive current. In the parameter space, the changes in synaptic weights increase the appearance of chimera states.

I. INTRODUCTION

In 1989, the coexistence of periodic and chaotic regimes in a dispersively coupled chain of oscillators was observed by Umberger *et al.*[1] In 2002, Kuramoto and Battogtokh[2] reported spatiotemporal patterns with coexisting coherence and incoherence domains in nonlocally coupled Ginzburg–Landau oscillators. In 2004, Abrams and Strogatz[3] named these above patterns with the coexistence of coherent and incoherent dynamics as chimera states.

Chimera states have been found in several physical, biological, and chemical systems.[4] Martens *et al.*[5] demonstrated the emergence of chimeras in mechanical oscillator networks. They devised an experiment with identical metronomes coupled by means of adjustable springs. In dolphins and birds, spatiotemporal patterns with different dynamics coexisting simultaneously might play a role in the situation in which one cerebral hemisphere sleeps while the other remains awake.[6] Tinsley *et al.*[7] reported subpopulations of coupled chemical oscillators with synchronized and desynchronized states. Experiments with a network of photosensitive chemical oscillators were carried out by Totz *et al.*[8] Numerical simulations and mathematical analysis have been used to study chimeras in network models. Santos *et al.*[9] explored the basin of attraction properties and its boundaries for chimera states. It was identified with fractal and riddled basin boundaries.

States of coexistence of synchronous and asynchronous patterns have attracted the attention of researchers that study neuronal systems. Haugland *et al.* highlighted the basic notion of chimera states as a combination of synchronous and asynchronous patterns.[10] Chimeras states have been observed in experimental coupled-map lattices.[11] Olmi *et al.*[12] found chimeras in coupled populations of leaky integrate-and-fire neurons. The coexistence of both coherent and incoherent groups of coupled Morris–Lecar neurons was identified by Calim *et al.*[13] Synchronous spatiotemporal patterns were observed in coupled Hindmarsh–Rose neurons[14,15] and also in networks of Hodgkin–Huxley neurons.[16] Santos *et al.*[17] demonstrated the coexistence of synchronous and asynchronous domains in a network composed of adaptive exponential integrate-and-fire neurons connected by means of chemical synapses.[18] Wang *et al.*[19] reported burst-timing dependent plasticity generating different evolutions of chimera states when compared to the static neuronal network. Majhi *et al.*[20] reported that chimera research focuses on some different aspects of neuronal networks as well as their relevance for physical and biological systems. Wolfram *et al.*[21] discussed the spectral properties of chimera states and highlighted a possible hyperchaotic nature of such phenomena. Chimera is present in nonlinear networks, brain networks without plasticity,[22] and Kuramoto-like networks with[23] and without plasticity.[24]

A simple description of neuronal plasticity is the capability of the synapses to change their intensity.[25] Phenomenological models of plasticity have been based on the rate or time of spikes.[26] In the rate models, the firing frequencies of the pre and postsynaptic neurons determine the intensity of the synaptic modification. On the other hand, in the spike timing models, the modifications depend on the spike time of the neurons sharing the synapses.[27] To study neuronal synchronization, plastic models that take into account the time dependency have been recurrently used. A particular rule to guide synaptic changes is the spike timing-dependent plasticity (STDP),[28] in which the changes of the synaptic connections depend on the spike time of the pre and postsynaptic neurons. Borges *et al.*[29] showed that the STDP rule can generate a preferential attachment from high to low spike frequency excitatory neurons. A rich club phenomenon was found in a neuronal network due to plasticity.[30] Another plasticity rule is the burst-timing dependent plasticity,[31] which is based on the burst start time between pre and post synaptic neurons. This plasticity is capable to induce synchronous and asynchronous clusters, each one operating in different frequencies.[32]

To study the chimera state neuronal plasticity, we build a regular network with plasticity composed of coupled adaptive exponential integrate-and-fire neurons (AEIF). The AEIF neuron[33] has an exponential mechanism of spike and an adaptation current, which modulates the neuron excitability dependent on the spikes. This neuron model is able to mimic various firing patterns in response to inputs. In this work, we explore the emergence of chimera states due to spike timing-dependent plasticity. We show that spike timing-dependent plasticity can induce chimera states in a one dimensional regular network where the synaptic weights are initially homogeneous. The chimera's lifetime increases with plasticity. Moreover, in the parameter space, we observe an increase in the neuronal firing frequency due to the changes in the synaptic weights and the emergence of chimera states.

This paper is organized as follows: Sec. II introduces the neuronal network of coupled AEIF neurons and the STDP rule. In Sec. III, we present the local order parameter, the coefficient of variation, and the mean firing frequency. In Sec. IV, we show the effects of plasticity in the emergence of chimera states. In the last section, we draw our conclusions and provide an outlook for future work.

II. METHODS

A. Neuronal network

We build a one-dimensional network composed of $N = 400$ AEIF neurons[33] locally coupled by means of excitatory chemical synapses, excluding auto-connections.[34] The boundary condition is periodic, i.e., the neuron $j = 1$ is a neighbor of the neuron $j = 400$ and vice versa. The neurons are connected to the R nearest neighbors according to a regular topology. In our simulations, we consider r as the normalized number of neighbors of neuron j on the left and right as $r = R/N$.

Each neuron's dynamics in the network are described by the following equations:

$$\begin{aligned} C_{\mathrm{m}}\frac{dV_j}{dt} &= -g_{\mathrm{L}}(V_j - E_{\mathrm{L}}) + g_{\mathrm{L}}\Delta_{\mathrm{T}}\exp\left(\frac{V_j - V_{\mathrm{T}}}{\Delta_{\mathrm{T}}}\right) - w_j \\ &\quad + I_0 + (V_{\mathrm{REV}} - V_j)\sum_{k=j-R}^{j+R} g_k M_{jk}, \\ \tau_w\frac{dw_j}{dt} &= a(V_j - E_{\mathrm{L}}) - w_j, \\ \tau_{\mathrm{s}}\frac{dg_j}{dt} &= -g_j, \end{aligned} \tag{1}$$

where V_j, w_j, and g_j correspond to the neuron variables membrane potential, adaptation current, and normalized synaptic conductance of neuron j, respectively. The constant parameters are C_{m} (membrane capacitance), g_{L} (leak conductance), E_{L} (resting potential), Δ_{T} (slope factor), V_{T} (spike threshold potential), I_0 (constant current applied), V_{REV} (synaptic reversal potential), V_{r} (reset potential), τ_w (adaptation time constant), a (sub-threshold adaptation level), b (over-threshold adaptation current), and τ_{s} (synaptic time constant). Initially, the weighted adjacency matrix M_{jk} has elements with values equal to M_{ex} when the presynaptic (k) and postsynaptic (j) neurons are connected and 0 when they are unconnected. The non-null connections ($M_{ij} = M_{\mathrm{ex}}$) can be or not be changed due to the plasticity rule, while null connections ($M_{ij} = 0$) are not changed. In our simulations, we consider $C_{\mathrm{m}} = 200$ pF, $E_{\mathrm{L}} = -70$ mV, $g_{\mathrm{L}} = 12$ nS, $\Delta_{\mathrm{T}} = 2$ mV, $V_{\mathrm{T}} = -50$ mV, $\tau_{\mathrm{w}} = 300$ ms, $a = 2$ nS, $\tau_{\mathrm{s}} = 1.5$ ms, $I_0 = 500$ pA, and $V_{\mathrm{REV}} = 0$ mV. When the membrane potential of neuron j is above the threshold potential, namely $V_j > V_{\mathrm{thres}}$,[35] we consider that a spike occurs and the variable of neuron j is updated. The V_j, w_j, and g_j variables are updated following the reset rule:

$$\begin{aligned} V_j &\to V_{\mathrm{r}}, \\ w_j &\to w_j + b, \\ g_j &\to 1, \end{aligned}$$

where $V_{\mathrm{r}} = -58$ mV and $b = 70$ pA. The initial intensity of the excitatory synaptic weight is given by M_{ex}. The initial conditions of the neuronal variables are randomly chosen in the range

$V_j = [-70, -50]$ mV and $w_j = [200, 400]$ pA. The initial normalized synaptic conductance of each neuron j (g_j) is equal to 0.

B. Spike time-dependent plasticity

Spike time-dependent plasticity (STDP) is a process that changes the synaptic strengths depending on the neuron spike time. For each synaptic connection, the spike time of the pre and post-synaptic neurons are identified as t_k and t_j, respectively. When $V_k > V_{\text{thres}}$, a spike occurs, and the reset rule is applied.

Depending on the time difference $\Delta t_{jk} = t_j - t_k$, the change in the synaptic weights ΔM_{jk} is given by[36,37]

$$\Delta M_{jk} = \begin{cases} A_1 e^{(-\Delta t_{jk}/\tau_1)} & \text{if } \Delta t_{jk} \geq 0, \\ -A_2 e^{(\Delta t_{jk}/\tau_2)} & \text{if } \Delta t_{jk} < 0, \end{cases} \tag{2}$$

where $A_1 = 1$, $A_2 = 0.5$, $\tau_1 = 1.8$ ms, and $\tau_2 = 6$ ms. The synaptic weights are updated according to Eq. (2), where $M_{jk} \to M_{jk} + 10^{-3}\Delta M_{jk}$. In our simulations, the synaptic weight represented by each matrix element is restricted in the interval $M_{ij} = [0, 1]$.

III. DIAGNOSTICS

A. Synchronous and asynchronous regions

As a diagnostic tool to identify synchronous and asynchronous behaviors, we utilized the local order parameter that is given by

$$z_j(t) = \frac{1}{2\delta + 1}\left|\sum_{k=j-\delta}^{j+\delta} e^{i\phi_k(t)}\right|, \tag{3}$$

where $2\delta + 1$ is the size region with the neuron j in the center ($\delta = 0.025N$).[38] The neurons are different, and then, it is impossible to observe a complete synchronization. As a consequence, the order parameter does not return a value equal to 1. Due to this fact, we assume that the neurons are synchronized when $z_j > 0.95$. The phase of each neuron k is defined as

$$\phi_k(t) = 2\pi l + 2\pi \frac{t - t_k^l}{t_k^{l+1} - t_k^l}, \tag{4}$$

where t_k^l is the time of the lth spike and $\phi_k(t)$ is defined in the interval $[t_k^l, t_k^{l+1}]$.

B. Chimera states

The chimera states are the coexistence of a group of synchronized oscillators with a group of desynchronized oscillators. To realize the analyses, we consider a threshold for high synchronous patterns. In this way, as presented in the literature, neuronal dynamics with $R > 0.9$ exhibit high synchronous patterns.[17,18] To diagnose the chimera states, we consider necessary at least one j with local order parameter $z_j > 0.9$ (synchronized) and at least one k with $z_k < 0.9$ (desynchronized), where $j, k \in [1, N]$.

We consider chimera states when synchronized and desynchronized patterns coexist in the time for more than half of the time simulation, i.e., when the chimera pattern is a predominantly pattern. The probability of chimera is taken into account, considering the number of initial conditions that present predominantly chimeras states over time. We define the chimera probability by

$$p_{\text{ch}} = \frac{N_{\text{ch}}}{N_{\text{ic}}}, \tag{5}$$

where N_{ch} is the number of times in which chimeras are predominant in the total number of initial conditions in our simulations (N_{ic}).

C. Mean firing frequency

We calculate the mean firing frequency of each neuron j by means of the corresponding inverse of the mean inter-spike intervals. The inter-spike intervals are defined as the time difference of consecutive spike times of the same neuron. Given the lth and $(l+1)$th spike times of a neuron j, the lth inter-spike interval of this neuron corresponds to $\text{ISI}_j^l = t_j^{l+1} - t_j^l$. In terms of $\overline{\text{ISI}}_j$, the mean frequency of the neuron j is given by $f_j = 1/\overline{\text{ISI}}_j$. Typically, in chimera states, incoherent regions have a larger frequency value than coherent ones.[3,39,40] In addition, we also compute the mean frequency for the entire network using $f_M = N^{-1}\sum_{j=1}^{N} f_j$.

IV. CHIMERA STATES INDUCED BY PLASTICITY

Figure 1 shows the neuronal dynamics for $r = 0.01$ and $M_{\text{ex}} = 0.01$ nS. The raster plot of V_j in Fig. 1(a) displays that the spike times are desynchronized over time. In Figs. 1(b) and 1(c), we see the snapshot of the action potential and the mean firing frequency of the jth neurons, respectively. The asynchronous spikes practically do not change the firing frequency in our simulation time. We observe only small changes in the mean firing frequency of each neuron, as a consequence of the small initial intensity and amount of neuron connections.

Figure 2 displays the existence of chimera for $r = 0.1$ and $M_{\text{ex}} = 0.07$ nS. In the raster plot [Fig. 2(a)] and potential snapshot

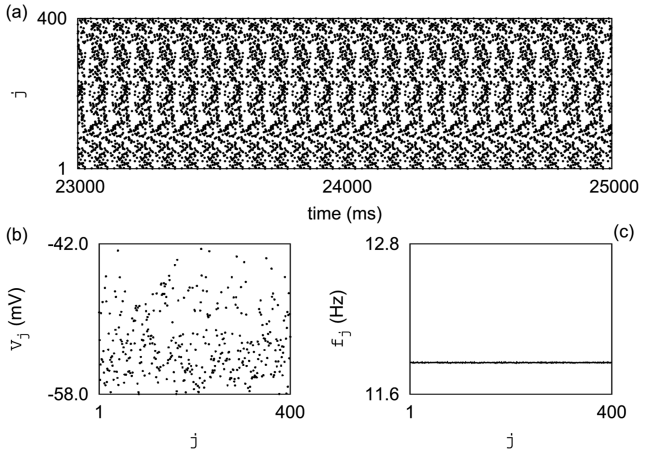

FIG. 1. Desynchronized pattern of coupled neurons. (a) Raster plot of V_j (spike times), (b) snapshot of $V_j(t)$, and (c) mean firing frequency of each neuron j for $r = 0.01$ and $M_{\text{ex}} = 0.01$.

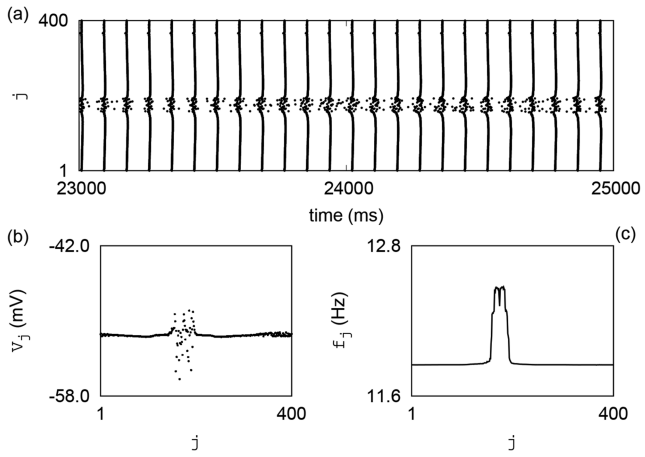

FIG. 2. Chimera states in a neuronal network for $r = 0.1$ and $M_{ex} = 0.07$. (a) Raster plot, (b) snapshot of $V_j(t)$, and (c) mean firing frequency of each neuron j.

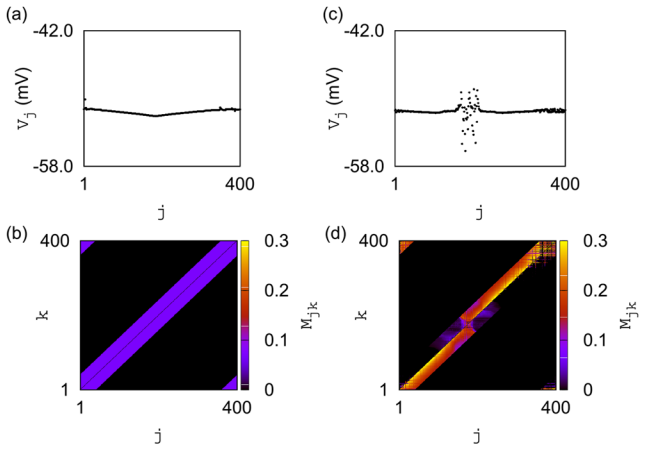

FIG. 4. $V_j \times j$ and weighted adjacency matrix for $r = 0.1$ and $M_{ex} = 0.07$. Panels (a) and (b) show our results for the neuronal network without plasticity and panels (c) and (d) for the network with STDP.

[Fig. 2(b)], it is possible to identify the coexistence of synchronized and desynchronized neuronal patterns. The mean firing frequency for the jth neurons [Fig. 2(c)] shows that the incoherent region has a higher frequency than the coherent one.

We investigate if synaptic plasticity could play a role in the appearance of chimera states. We find the regions in the parameter space $(r \times M_{ex})$ where the chimeras appear and compute the chimera probability to compare the results with and without synaptic plasticity, as shown in Fig. 3. Figures 3(a) and 3(b) display the values of r and M_{ex} in which chimeras emerge for the cases without and with STDP, respectively. In Figs. 3(c) and 3(d), we calculate the probability to obtain chimera states in the network without and with synaptic plasticity rule, respectively. We consider $t_f = 30$ s with a transient time $t_r = 20$ s. As demonstrated in Fig. 3, due to the plasticity, there is an increase in the region size in which the chimera states are found. For a probability equal to 1, the chimera states appear for all considered initial conditions.

To analyze the differences between the dynamics without and with plasticity, we consider a potential profile and synaptic coupling matrix for a case in which the plasticity changes considerably in the network dynamics. Figures 4(a) and 4(c) exhibit the spatial profile of V_j, while Figs. 4(b) and 4(d) display the coupling matrix for $r = 0.1$ and $M_{ex} = 0.07$. Without plasticity (left panels), for the considered initial conditions, the synaptic couplings are homogeneous and generate synchronized states. However, when the plasticity is active in the neuronal network, the synaptic coupling intensities change and go from homogeneity to heterogeneity. In the synchronized regions, it is possible to observe a predominant directional reinforcement of the connections, as shown in Figs. 4(c) and 4(d). For two neurons j_1 and j_2 localized in the synchronized region, we observe

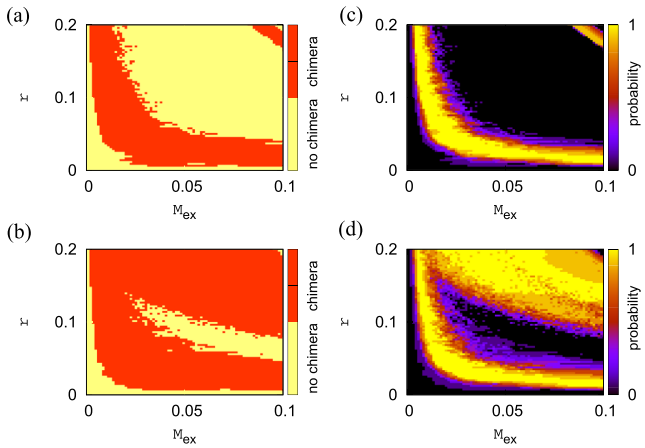

FIG. 3. Parameter space of $r \times M_{ex}$ without [(a) and (c)] and with [(b) and (d)] plasticity. We consider $N = 400$, $t_f = 30$ s, $t_r = 20$ s, and 11 different initial conditions. The left panels show the red regions where there are chimera states and the right panels display the chimeras' probability.

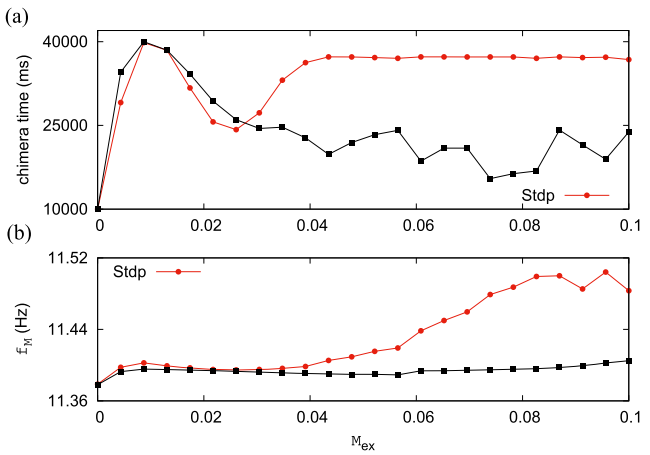

FIG. 5. (a) Chimera lifetime and (b) average network frequency (f_M) for $r = 0.1$, where the red and black lines correspond to the neuronal network with and without STDP.

potentiation from j_1 to j_2 or j_2 to j_1, while depression occurs in another direction. A similar potentiation and depression mechanism occurs between neurons from high to low frequencies.[29] When the synchronization is not completely in phase, as the neurons $i, j = [350, 400]$ in Figs. 4(c) and 4(d), complex configurations of potentiation and depression can occur.[41]

In Fig. 5(a), we compute the chimera lifetime with (red line) and without (black line) STDP. The time between the formation of the chimera state and the collapse of the synchronized state is larger for the network with STDP than without plasticity. The plasticity is able to increase the chimera lifetime. It is also possible to notice an increase in the average network frequency (f_M) due to the coexistence of states in the spatial profile, as displayed in Fig. 5(b).

V. CONCLUSIONS

In this work, we investigate the effect of spike timing-dependent plasticity (STDP) in the appearance of chimera states. We consider a one-dimensional regular neuronal network in which each element is described by the adaptive exponential integrate-and-fire neuron. To generate the spikes, we consider a positive constant current in all neurons.

In the absence of plasticity, chimera states have been observed in regular networks. We find that STDP is able to induce chimera states for a more broad parameters set. The plasticity rule increases the regions in the parameter space ($M_{\text{ex}} \times r$) where chimeras emerge when compared with the case without plasticity. Furthermore, the chimera lifetime increases due to the STDP rule. In addition, we also observe the increase of the mean firing frequency as a consequence of the plasticity in a region of large initial synaptic weight. Based on previous studies,[19,42–44] we believe that longer chimera states can be provided by the synaptic weight heterogeneity as well as no static synaptic weights.

Our results could be limited to the time considered in the simulation. For a long time, we suspect that there are parameter regions where chimera states appear and disappear in an intermittent and complex way. In future works, we plan to explore this dynamic behavior for a long time and deep into the comprehension between firing patterns and synaptic changes. We also expect to investigate how the initial network configuration can impact the chimera emergence in the presence of plasticity.

ACKNOWLEDGMENTS

This study was supported by the National Natural Science Foundation of China (Grant Nos. 11875133, 11075057, and 12147101). This study was also possible by partial financial support from the following Brazilian government agencies: Fundação Araucária, National Council for Scientific and Technological Development (CNPq), Coordenação de Aperfeiçoamento de Pessoal de Nível Superior—Brasil (CAPES), and São Paulo Research Foundation (FAPESP) (Grant Nos. 2018/03211-6 and 2020/04624-2).

AUTHOR DECLARATIONS

Conflict of Interest

The authors have no conflicts to disclose.

Author Contributions

C.Y. and M.S.S. contributed equally to this work.

Chao Yang: Formal analysis (equal); Funding acquisition (equal); Investigation (equal); Methodology (equal); Writing – original draft (equal). **Moises S. Santos**: Conceptualization (equal); Formal analysis (equal); Investigation (equal); Methodology (equal); Writing – original draft (equal). **Paulo R. Protachevicz**: Conceptualization (equal); Formal analysis (equal); Investigation (equal); Writing – original draft (equal). **Patrício D. C. dos Reis**: Investigation (equal); Methodology (equal). **Kelly C. Iarosz**: Formal analysis (equal); Investigation (equal); Methodology (equal). **Iberê L. Caldas**: Supervision (equal); Validation (equal). **Antonio M. Batista**: Investigation (equal); Supervision (equal).

DATA AVAILABILITY

The data that support the findings of this study are available from the corresponding author upon reasonable request.

REFERENCES

[1] D. K. Umberger, C. Grebogi, E. Ott, and B. Afeyan, "Spatiotemporal dynamics in a dispersively coupled chain of nonlinear oscillators," Phys. Rev. A **39**, 4835 (1989).
[2] Y. Kuramoto and D. Battogtokh, "Coexistence of coherence and incoherence in nonlocally coupled phase oscillators," Nonlinear Phenom. Complex Syst. **5**, 380–385 (2002).
[3] D. M. Abrams and S. H. Strogatz, "Chimera states for coupled oscillators," Phys. Rev. Lett. **93**, 174102 (2004).
[4] R. Middya and A. R. Chowdhury, "Chimera states—A brief introduction," Res. Dev. Mater. Sci. **6**, 532 (2018).
[5] E. A. Martens, S. Thutupalli, A. Fourrière, and O. Hallatschek, "Chimera states in mechanical oscillators networks," Proc. Natl. Acad. Sci. U. S. A. **110**, 10563 (2013).
[6] N. C. Rattenborg, C. J. Amlaner, and S. L. Lima, "Behavioral, neurophysiological and evolutionary perspectives on unihemispheric sleep," Neurosci. Biobehav. Rev. **24**, 817 (2000).
[7] M. R. Tinsley, S. Nkomo, and K. Showalter, "Chimera and phase-cluster states in populations of coupled chemical oscillators," Nat. Phys. **8**, 662 (2012).
[8] J. F. Totz, J. Rode, M. R. Tinsley, K. Showalter, and H. Engel, "Spiral wave chimera states in large populations of coupled chemical oscillators," Nat. Phys. **14**, 282 (2018).
[9] V. Santos, J. D. Szezech, Jr., A. M. Batista, K. C. Iarosz, M. S. Baptista, H. P. Ren, C. Grebogi, R. L. Viana, I. L. Caldas, Y. L. Maistrenko, and J. Kurths, "Riddling: Chimera's dilemma," Chaos **28**, 081105 (2018).
[10] S. W. Haugland,"The changing notion of chimera states, a critical review," J. Phys.: Complexity **2**, 032001 (2021).
[11] A. M. Hagerstrom, T. E. Murphy, R. Roy, P. Hövel, I. Omelchenko, and E. Schöll, "Experimental observation of chimeras in coupled-map lattices," Nat. Phys. **8**, 658–661 (2012).
[12] S. Olmi, A. Politi, and A. Torcini, "Collective chaos in pulse-coupled neural networks," Europhys. Lett. **92**, 60007 (2010).
[13] A. Calim, P. Hövel, M. Ozer, and M. Uzuntarla, "Chimera states in networks of type-I Morris-Lecar neurons," Phys. Rev. E **98**, 062217 (2018).
[14] J. Hizanidis, N. E. Kouvaris, G. Zamora-López, A. Díaz-Guilera, and C. G. Antonopoulos, "Chimera-like states in modular neural networks," Sci. Rep. **6**, 19845 (2016).
[15] M. S. Santos, J. D. Szezech, F. S. Borges, K. C. Iarosz, I. L. Caldas, A. M. Batista, R. L. Viana, and J. Kurths, "Chimera-like states in a neuronal network model of the cat brain," Chaos, Solitons and Fractals **101**, 86 (2017).

[16]T. A. Glaze, S. Lewis, and S. Bahar, "Chimera states in a Hodgkin-Huxley model of thermally sensitive neurons," Chaos **26**, 083119 (2016).
[17]M. S. Santos, P. R. Protachevicz, K. C. Iarosz, I. L. Caldas, R. L. Viana, F. S. Borges, H.-P. Ren, J. D. Szezech, Jr., A. M. Batista, and C. Grebogi, "Spike-burst chimera states in an adaptive exponential integrate-and-fire neuronal network," Chaos **29**, 043106 (2019).
[18]M. S. Santos, P. R. Protachevicz, I. L. Caldas, K. C. Iarosz, R. L. Viana, J. D. Szezech, Jr., S. L. T. de Souza, and A. M. Batista, "Spiral wave chimera states in regular and fractal neuronal networks," J. Phys.: Complexity **2**, 015006 (2021).
[19]Z. Wang, S. Baruni, F. Parastesh, S. Jafari, D. Ghosh, M. Perc, and I. Hussain, "Chimeras in an adaptive neuronal network with burst-timing-dependent plasticity," Neurocomputing **406**, 117–126 (2020).
[20]S. Majhi, B. K. Bera, D. Ghosh, and M. Perc, "Chimera states in neuronal networks: A review," Phys. Life Rev. **28**, 100–121 (2019).
[21]M. Wolfrum, O. E. Omel'chenko, S. Yanchuk, and Y. L. Maistrenko, "Spectral properties of chimera states," Chaos **21**, 013112 (2011).
[22]Z. Wang and Z. Liu, "A brief review of chimera state in empirical brain networks," Front. Physiol. **11**, 1–16 (2020).
[23]A. E. Botha, M. Ansariara, S. Emadi, and M. R. Kolahchi, "Chimera patterns of synchrony in a frustrated array of Hebb synapses," Front. Comput. Neurosci. **16**, 1–15 (2022).
[24]A. Lucchetti, M. H. Jensen, M. L. Heltberg, "Emergence of chimera states in a neuronal model of delayed oscillators," Phys. Rev. Res. **3**, 033041 (2021).
[25]A. Citri and R. C. Malenka, "Synaptic plasticity: Multiple forms functions and mechanisms," Neuropsychopharmacology **33**, 18–41 (2008).
[26]W. Gerstner and W. Kistler, *Spiking Neuron Models: Single Neurons, Populations, Plasticity* (Cambridge University Press, Cambridge, 2002).
[27]A. Morrison, M. Diesmann, and W. Gerstner, "Phenomenological models of synaptic plasticity based on spike time," Biol. Cybern. **98**, 459–478 (2008).
[28]G.-q. Bi and M.-m. Poo, "Synaptic modification by correlated activity: Hebb's postulate revisited," Annu. Rev. Neurosci. **24**, 139–166 (2001).
[29]R. R. Borges, F. S. Borges, E. L. Lameu, A. M. Batista, K. C. Iarosz, I. L. Caldas, C. G. Antonopoulos, and M. S. Baptista, "Spike timing-dependent plasticity induces non-trivial topology in the brain," Neural Networks **88**, 58–64 (2017).
[30]R. R. Borges, F. S. Borges, E. L. Lameu, P. R. Protachevicz, K. C. Iarosz, I. L. Caldas, R. L. Viana, E. E. N. Macau, M. S. Baptista, C. Grebogi, and A. M. Batista, "Synaptic plasticity and spike synchronization in neuronal networks," Braz. J. Phys. **47**, 678–688 (2017).
[31]D. A. Butts, P. O. Kanold, and C. J. Shatz, "A burst-based 'Hebbian' learning rule at retinogeniculate synapses links retinal waves to activity-dependent refinement," PLoS Biol. **5**, e61 (2007).
[32]J. A. Paludo Silveira, P. R. Protachevicz, R. L. Viana, and A. M. Batista, "Effects of burst-timing-dependent plasticity on synchronous behaviour in neuronal network," Neurocomputing **436**, 126–135 (2021).
[33]R. Brette and W. Gerstner, "Adaptive exponential integrate-and-fire model as an effective description of neuronal activity," J. Neurophysiol. **94**, 3637–3642 (2005).
[34]P. R. Protachevicz, K. C. Iarosz, I. L. Caldas, C. G. Antonopoulos, A. M. Batista, and J. Kurths, "Influence of autapses on synchronization in neural networks with chemical synapses," Front. Syst. Neurosci. **14**, 91 (2020).
[35]R. Naud, N. Marcille, C. Clopath, and W. Gerstner, "Firing patterns in the adaptive exponential integrate-and-fire model," Biol. Cybern. **99**, 335–347 (2008).
[36]G. Q. Bi and M. M. Poo, "Synaptic modifications in cultured hippocampal neurons: Dependence on spike timing, synaptic strength, and postsynaptic cell type," J. Neurosci. **18**, 10464–10472 (1998).
[37]O. V. Popovych, S. Yanchuk, and P. A. Tass, "Self-organized noise resistance of oscillatory neural networks with spike timing-dependent plasticity," Sci. Rep. **3**, 2926 (2013).
[38]I. Omelchenko, Y. Maistrenko, P. Hövel, and E. Schöll, "Loss of coherence in dynamical networks: Spatial chaos and chimera states," Phys. Rev. Lett. **106**, 234102 (2011).
[39]F. S. Borges, P. R. Protachevicz, E. L. Lameu, R. C. Bonetti, K. C. Iarosz, I. L. Caldas, M. S. Baptista, and A. M. Batista, "Synchronized firing patterns in a random network of adaptive exponential integrate-and-fire neuron model," Neural Networks **90**, 1–7 (2017).
[40]M. Wolfrum and O. E. Omel'chenko, "Chimera states are chaotic transients," Phys. Rev. E **84**, 015201 (2011).
[41]E. L. Lameu, E. E. N. Macau, F. S. Borges, K. C. Iarosz, I. L. Caldas, R. R. Borges, P. R. Protachevicz, R. L. Viana, and A. M. Batista, "Alternations in brain connectivity due to plasticity and synaptic delay," Eur. Phys. J. **227**, 673–682 (2018).
[42]C. R. Laing, "Chimera states in heterogeneous networks," Chaos **19**, 013113 (2009).
[43]B. Li and D. Saad, "Chimera-like states in structure heterogeneous networks," Chaos **27**, 043109 (2017).
[44]S. Huo, C. Tian, L. Kang, and Z. Liu, "Chimera states of neuron networks with adaptive coupling," Nonlinear Dyn. **96**, 75–86 (2019).